Acta Crystallographica Section D
Biological Crystallography
ISSN 0907-4449

Crystallization and preliminary X-ray analysis of the EVH1 domain of Vesl-2b

Melanie Barzik,[a] Wolf-Dieter Schubert,[a] Uwe Carl,[b] Jürgen Wehland[b] and Dirk W. Heinz[a]*

[a]Department of Structural Biology, German National Center of Biotechnology (GBF), Mascheroder Weg 1, D-38124 Braunschweig, Germany, and [b]Department of Cell Biology, German National Center of Biotechnology (GBF), Mascheroder Weg 1, D-38124 Braunschweig, Germany

Correspondence e-mail: dirk.heinz@gbf.de

Received 8 March 2000
Accepted 12 April 2000

Proteins of the Homer/Vesl family are enriched at excitatory synapses and selectively bind to a proline-rich consensus sequence in group 1 metabotropic glutamate receptors *via* a domain that shows a strong similarity to the Ena/VASP homology 1 (EVH1) domains. EVH1 domains play an important role in actin cytoskeleton dynamics. Crystals of the EVH1 domain of murine Vesl-2b were obtained that diffract X-rays to 2.4 Å resolution. They belong to space group *C*2, with unit-cell parameters $a = 112.8$, $b = 69.9$, $c = 54.9$ Å, $\beta = 110.7^\circ$, consistent with three molecules per asymmetric unit and a solvent content of 53%.

1. Introduction

Recently, a family of adaptor proteins, including *Drosophila* Enabled (Ena), mammalian vasodilator-stimulated phosphoprotein (VASP) and Wiskott–Aldrich syndrome protein (WASP), has been implicated in the spatial coordination of proteins involved in the actin-assembly machinery (Pollard, 1995; Machesky, 1997; Beckerle, 1998). All family members contain an N-terminal protein-interaction module referred to as Enabled/VASP homology 1 (EVH1) domain (Gertler *et al.*, 1996; Symons *et al.*, 1996; Ponting & Phillips, 1997). EVH1 domains participate in directed cell movement by recruiting proteins to sites of actin dynamics. EVH1 domains specifically recognize proline-rich motifs of the consensus sequence FPPPP (Niebuhr *et al.*, 1997). This motif is not only found in proteins involved in transmitting external signals to the actin cytoskeleton (Reinhard *et al.*, 1995; Niebuhr *et al.*, 1997; Machesky & Insall, 1998), but also tandemly repeated in the protein ActA from the human pathogen *Listeria monocytogenes* (Chakraborty *et al.*, 1995; Gertler *et al.*, 1996; Smith *et al.*, 1996). The crystal structures of the EVH1 domains of mammalian Ena (Prehoda *et al.*, 1999) and Ena/VASP-like protein (Fedorov *et al.*, 1999) have been shown to be strikingly similar to pleckstrin homology (PH) and phosphotyrosine-binding protein (PTB) domains (reviewed by Blomberg *et al.*, 1999). The structures which were obtained in complex with their target peptides also demonstrated that these interaction modules utilize a mechanism of proline-motif recognition that is primarily based on the conformational properties of the ligand, *i.e.* a polyproline II (PPII) conformation, rather than the specific identity of residues. The PPII conformation is a left-handed helix with three residues per turn.

Interestingly, EVH1 domains are also found in a distinct class of proteins with no obvious link to the actin cytoskeleton. These proteins belong to the Homer/Vesl family of post-synaptic proteins which play an important role in synaptic plasticity and long-term potentiation (Brakeman *et al.*, 1997; Kato *et al.*, 1997). There is a sequence identity of about 30% between Homer/Vesl and Mena/VASP protein families (Callebaut *et al.*, 1998; Prehoda *et al.*, 1999). The Homer/Vesl EVH1 domains specifically recognize the proline-rich motif PPSPF located in the C-terminal region of group 1 metabotropic glutamate receptors (mGluRs; Xiao *et al.*, 1998) as well as the consensus motif

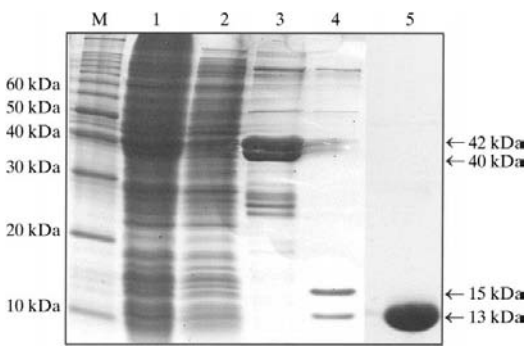

Figure 1
SDS–PAGE of mVesl-2b EVH1 domain expression and purification. M, molecular-weight marker; lane 1, soluble fraction; lane 2, glutathione Sepharose column eluate; lane 3, GST-mVesl-2b fusion proteins bound to glutathione Sepharose; lane 4, elution of 13 and 15 kDa mVesl-2b proteins after on-column cleavage with PreScission protease; lane 5, purified mVesl-2b EVH1 domain (residues 1–111).

PP*xx*F in inositol 1,4,5-triphosphate (IP_3) receptors (Tu *et al.*, 1998) and the post-synaptic density protein Shank (Tu *et al.*, 1999). The apparent reversal of the sequence motif (PPSPF instead of FPPPP) suggests that the EVH1 domain may recognize its natural ligand in the opposite orientation. A similar phenomenon has previously been observed for SH3 domains, which also recognize proline-rich sequences in two alternative orientations (Lim *et al.*, 1994; Musacchio *et al.*, 1994).

Here, we report the purification, crystallization and preliminary X-ray crystallographic analysis of the EVH1 domain (amino acids 1–111) of murine Vesl (mVesl-2b).

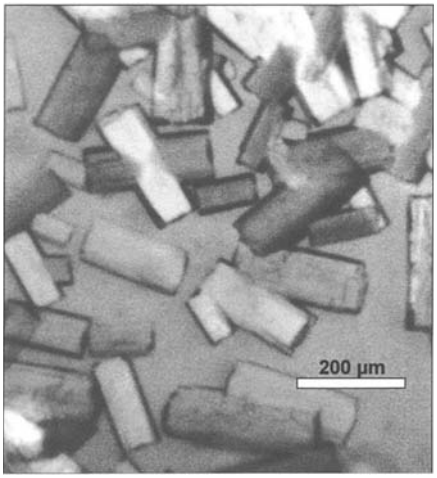

Figure 2
Crystals of the mVesl-2b EVH1 domain. Dimensions of the crystals are indicated by a scale bar.

2. Bacterial expression and purification

The coding sequence for the EVH1 domain of mVesl-2b (residues 1–118) was amplified using PCR and cloned into the *Nco*I/*Bam*HI sites of the *Escherichia coli* expression vector pGEX-6P-1 (Pharmacia). For expression, cells were grown at 310 K in LB medium containing 100 µg ml^{-1} ampicillin until an OD_{600} of 0.5–0.8 was reached. Prior to induction with isopropylthio-β-D-galactoside to a final concentration of 0.1 m*M*, cells were cooled to 293 K. Cell culturing was continued for 18 h. After cell lysis using a French press, the supernatant was applied to an equilibrated glutathione Sepharose column (Pharmacia). The column was extensively washed with PreScission protease cleavage buffer (Pharmacia) containing 50 m*M* Tris–HCl pH 7.0, 150 m*M* NaCl, 1 m*M* EDTA and 1 m*M* DTT. The glutathione-S-transferase fusion partner was removed by adding 200 units of PreScission protease (Pharmacia) and incubating at 277 K for 3–5 d. Cleaved mVesl-2b was eluted with PBS and concentrated using Centriplus 3 cells (Amicon). The protein was further purified by ion-exchange chromatography using a Mono S column (Pharmacia) and a linear NaCl gradient (0–1*M* NaCl in 20 m*M* HEPES pH 7.5). mVesl-2b-containing fractions were pooled and concentrated to 15 mg ml^{-1} protein. The protein concentration was estimated using a calculated extinction coefficient (Gill & von Hippel, 1989). The progress of protein purification was followed using SDS–PAGE.

Domain borders of the initial construct (residues 1–118) were chosen using sequence alignments (Callebaut *et al.*, 1998). Owing to the cloning strategy, the cleaved mVesl-2b protein contained five additional N-terminal amino-acid residues. Owing to the erroneous placement of a stop codon, 15 additional C-terminal amino-acid residues derived from the vector were attached to the C terminus. This protein (15 kDa) was, however, partially degraded in the *E. coli* cells to a smaller protein of about 13 kDa (Fig. 1). N-terminal amino-acid sequencing and MALDI–TOF mass spectrometry showed that the truncated version contained the first 111 amino acids of mVesl-2b plus five N-terminal amino acids from the expression vector. Because the smaller protein remained stable during purification, we concluded that residue 111 represents the last residue of the mVesl-2b EVH1 domain. Consequently, a new expression vector for the production of the first 111 mVesl-2b amino acids was constructed. Using this construct, we were able to

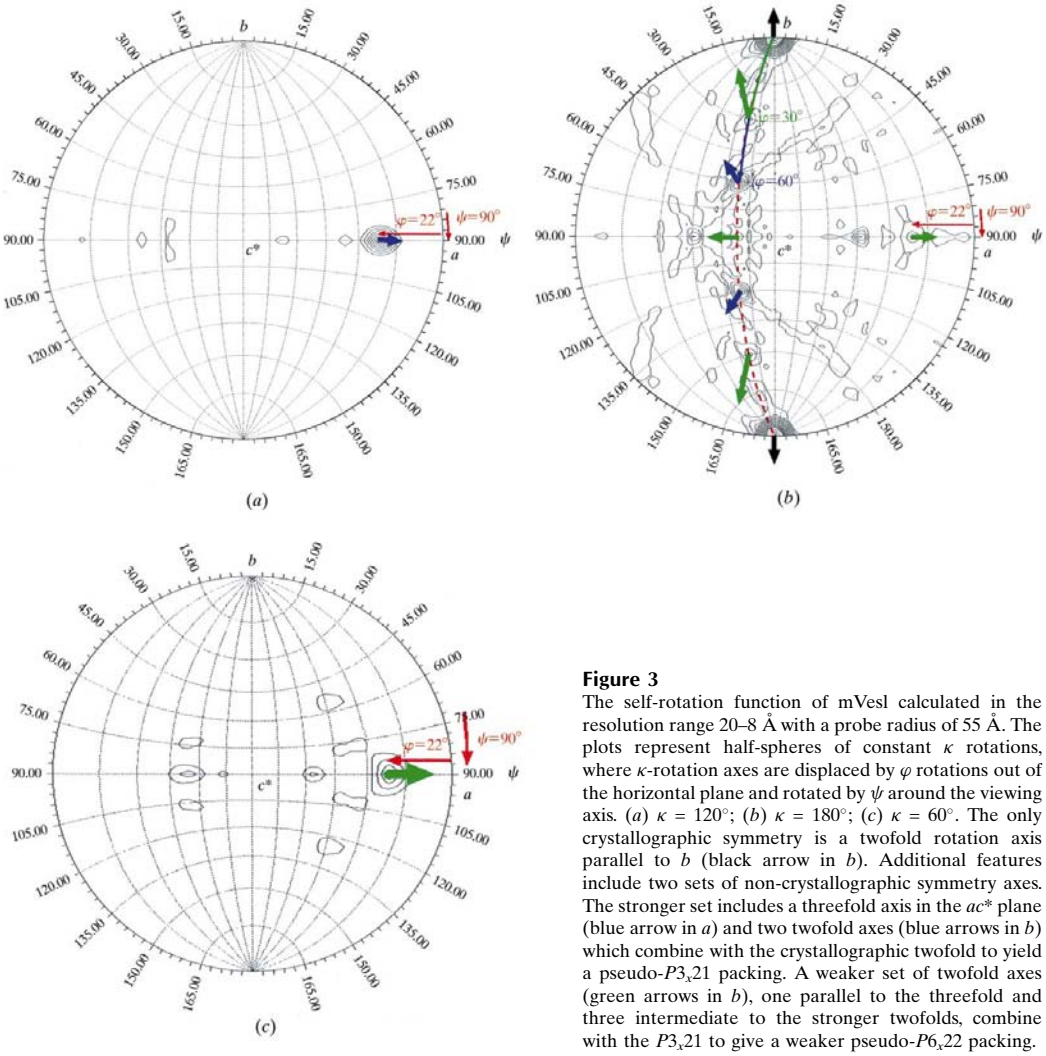

Figure 3
The self-rotation function of mVesl calculated in the resolution range 20–8 Å with a probe radius of 55 Å. The plots represent half-spheres of constant κ rotations, where κ-rotation axes are displaced by φ rotations out of the horizontal plane and rotated by ψ around the viewing axis. (*a*) κ = 120°; (*b*) κ = 180°; (*c*) κ = 60°. The only crystallographic symmetry is a twofold rotation axis parallel to *b* (black arrow in *b*). Additional features include two sets of non-crystallographic symmetry axes. The stronger set includes a threefold axis in the *ac** plane (blue arrow in *a*) and two twofold axes (blue arrows in *b*) which combine with the crystallographic twofold to yield a pseudo-$P3_x21$ packing. A weaker set of twofold axes (green arrows in *b*), one parallel to the threefold and three intermediate to the stronger twofolds, combine with the $P3_x21$ to give a weaker pseudo-$P6_x22$ packing.

purify the recombinant mVesl-2b EVH1 domain, yielding up to 30 mg protein per litre of bacterial culture. The protein was ≥99% pure as judged from Coomassie-blue stained SDS–PAGE (Fig. 1).

3. Protein crystallization

Prior to crystallization, the protein was dialysed against 20 m*M* HEPES pH 7.5. Sitting-drop crystallization experiments were performed at 293 K using Crystal Screens I and II and 96 well plates (Hampton Research, Laguna Hills, USA; Jancarik & Kim, 1991; Cudney *et al.*, 1994). 3 µl of protein solution (15 mg ml^{-1}) and 3 µl of precipitant solution were mixed and allowed to equilibrate against 100 µl of reservoir solution. Small crystals (<100 µm) were obtained from 1.6 *M* $(NH_4)_2SO_4$, 0.1 *M* NaCl, 0.1 *M* HEPES pH 7.5.

Further crystal optimization was performed by the hanging-drop vapour-diffusion method in Linbro plates by mixing 5 µl protein solution with 5 µl precipitant and equilibrating against 500 µl reservoirs. Crystal growth was optimized using additive- and detergent-screening kits (Hampton Research). The largest crystals, with dimensions of 0.3 × 0.2 × 0.2 mm (Fig. 2), were obtained by adding 1 µl of a 0.1 *M* solution of nicotinamide adenine dinucleotide (from the additive-screening kit) to the drop. Prior to data collection at 100 K, the crystals were cryoprotected by adding glycerol to a final concentration of 25%(*v*/*v*).

4. X-ray data collection and processing

A first X-ray data set was collected to 3.2 Å resolution using graphite-monochromated X-rays from a Nonius FR571 X-ray generator operated at 50 kV and 90 mA and a MAR 18 cm image plate (FU Berlin, Germany) at room temperature. Data were processed using the *HKL* package (Otwinowski & Minor, 1997). The space group of the crystals was *C*2, with unit-cell parameters $a = 115.2, b = 71.2, c = 55.7$ Å, $\beta = 109^\circ$. A self-rotation function was calculated using the program *GLRF* (Tong & Rossmann, 1997), using a resolution range of 20–8 Å and a Patterson cutoff radius of 55 Å. Apart from the crystallographic (monoclinic) twofold axis (20σ, $\kappa = 180^\circ$; black vertical arrow in Fig. 3*b*), the highest peak (7σ) in the self-rotation function is located on the $\kappa = 120^\circ$ section, indicating a non-crystallographic threefold axis in the *ac* plane offset from the *a* axis by about 22° (blue arrow in Fig. 3*a*). Interestingly, the non-crystallographic threefold axis is aligned with a weak twofold axis (2σ; Fig. 3*b*), giving rise to a similarly weak sixfold rotation axis (3σ, $\kappa = 60^\circ$; Fig. 3*c*). Roughly perpendicular to the threefold and sixfold axes, a set of two stronger twofold axes (5σ; blue arrows in Fig. 3*b*) are observed which complement the monoclinic twofold and the pseudo-threefold to give a non-crystallographic $P3_x21$ packing. In addition, weaker twofold axes (2σ; green arrows) intermediate to the stronger twofold axes combine with the weak sixfold axis to form a degenerate $P6_x22$ packing. This pseudo-hexagonal packing dominates the crystal morphology, though for some reason most crystallographic symmetry is lost, leaving only a monoclinic crystallographic symmetry.

To corroborate the discussion above, data reduction was repeated in *P*1 and the self-rotation function recalculated in an identical fashion (not shown). This confirms the presence of a single crystallographic twofold axis and progressively weaker $P3_x21$ and $P6_x22$ pseudo-packing.

Under the assumption of three protein molecules per asymmetric unit, a reasonable V_M value of 2.77 Å^3 Da^{-1}, corresponding to a solvent content of 55.3%, was calculated (Matthews, 1968).

A second complete data set (completeness = 96.2%, $R_{\rm merge}$ = 6.9%) was collected under cryogenic conditions to 2.4 Å using synchrotron radiation and a MAR CCD detector (Beamline BW6, DESY Hamburg, Germany) at 100 K. Structure determination using the selenomethionine-substituted protein and the MAD phasing method is currently in progress.

We thank the staff of the BW6 beamline (DESY Hamburg, Germany) for their help with data collection. The excellent technical assistance of Rita Getzlaff (amino-acid sequencing) and Dr Manfred Nimtz (mass spectrometry) is gratefully acknowledged. Finally we thank the 'Resource Centre of the German Human Genome Project' at the Max-Planck-Institute for Molecular Genetics (Berlin, Germany) for providing the EST clone (AA 491171; RZPD: IMAG p998L102036).

References

Beckerle, M. C. (1998). *Cell*, **95**, 741–748.
Blomberg, N., Baraldi, E., Nilges, M. & Saraste, M. (1999). *Trends Biochem. Sci.* **24**, 441–445.
Brakeman, P. R., Lanahan, A. A., O'Brien, R., Roche, K., Barnes, C. A., Huganir, R. L. & Worley, P. F. (1997). *Nature (London)*, **386**, 284–288.
Callebaut, I, Cossart, P. & Dehoux, P. (1998). *FEBS Lett.* **441**, 181–185.
Chakraborty, T., Ebel, F., Domann, E., Niebuhr, K., Gerstel, B., Pistor, S., Temm-Grove, C. J., Jockusch, B. J., Reinhard, M., Walter, U. & Wehland, J. (1995). *EMBO J.* **14**, 1314–1321.
Cudney, R., Patel, S., Weisgraber, K., Newhouse, Y. & McPherson, A. (1994). *Acta Cryst.* D**50**, 414–423.
Fedorov, A. A., Fedorov, E., Gertler, F. & Almo, S. C. (1999). *Nature Struct. Biol.* **6**, 661–665.
Gertler, F. B., Niebuhr, K., Reinhard, M., Wehland, J. & Soriano, P. (1996). *Cell*, **87**, 227–239.
Gill, S. C. & von Hippel, P. H. (1989). *Anal. Biochem.* **182**, 319–326.
Jancarik, J. & Kim, S.-H. (1991). *J. Appl. Cryst.* **24**, 409–411.
Kato, A., Ozawa, F., Saitoh, Y., Hirai, K. & Inokuchi, K. (1997). *FEBS Lett.* **412**, 183–189.
Lim, W. A., Richards, F. M. & Fox, R. O. (1994). *Nature (London)*, **372**, 375–379.
Machesky, L. M. (1997). *Curr. Biol.* **7**, R164–R167.
Machesky, L. M. & Insall, R. H. (1998). *Curr. Biol.* **31**, 1347–1356.
Matthews, B. W. (1968). *J. Mol. Biol.* **33**, 491–497.
Musacchio, A., Saraste, M. & Wilmanns, M. (1994). *Nature Struct. Biol.* **1**, 546–551.
Niebuhr, K., Ebel, F., Frank, R., Reinhard, M., Domann, E., Carl, U. D., Walter, U., Gertler, F. B., Wehland, J. & Chakraborty, T. (1997). *EMBO J.* **16**, 5433–5444.
Otwinowski, Z. & Minor, W. (1997). *Methods Enzymol.* **276**, 307–325.
Pollard, T. D. (1995). *Curr. Biol.* **5**, 837–840.
Ponting, C. P. & Phillips, C. (1997). *J. Mol. Med.* **75**, 769–771.
Prehoda, K. E., Lee, D. J. & Lim, W. A. (1999). *Cell*, **97**, 471–480.
Reinhard, M., Giehl, K., Abel, K., Haffner, C., Jarchau, T., Hoppe, V., Jockusch, B. M. & Walter, U. (1995). *EMBO J.* **14**, 1583–1589.
Smith, G. A., Theriot, J. A. & Portnoy, D. A. (1996). *J. Cell Biol.* **135**, 647–660.
Symons, M., Derry, J. M., Karlak, B., Jiang, S., Lemahieu, V., McCormick, F., Francke, U. & Abo, A. (1996). *Cell*, **84**, 723–734.
Tong, L. & Rossmann, M. G. (1997). *Methods Enzymol.* **276**, 594–611.
Tu, J. C., Xiao, B., Naisbitt, S., Yuan, J. P., Petralia, R. S., Brakeman, P. R., Doan, A., Aakalu, V. K., Lanahan, A. A., Sheng, M. & Worley, P. F. (1999). *Neuron*, **23**, 583–592.
Tu, J. C., Xiao, B., Yuan, J. P., Lanahan, A. A., Leoffert, K., Li, M., Linden, D. J. & Worley, P. F. (1998). *Neuron*, **21**, 717–726.
Xiao, B., Tu, J. C., Petralia, R. S., Yuan, J. P., Doan, A., Breder, C. D., Ruggerio, A., Lanahan, A. A., Wenthold, R. J. & Worley, P. F. (1998). *Neuron*, **21**, 707–716.